A range of 30–62% of functioning multiciliated airway cells is sufficient to maintain ciliary airway clearance

Niki T. Loges, June Kehlet Marthin ⓘ, Johanna Raidt, Heike Olbrich, Inga M. Höben, Sandra Cindric, Diana Bracht, Julia König ⓘ, Cynthia Rieck, Sebastian George, Tim Luis Kloth, Kai Wohlgemuth, Petra Pennekamp, Bernd Dworniczak, Mathias G. Holgersen ⓘ, Jobst Römel ⓘ, Christian Schmalstieg, Isabella Aprea, Jann Mortensen, Kim G. Nielsen and Heymut Omran ⓘ

	How many functional multiciliated airway cells are sufficient to maintain ciliary airway clearance?		
Studied individuals	Healthy male individuals (n=5) — X Y DNAAF6; Healthy female individuals (n=26) — X X DNAAF6	Male PCD individuals (n=5) — X Y, No X-chromosome inactivation, Pathogenic variant, Progenitor cell	Female carriers (n=6) — X X, Random X-chromosome inactivation, Pathogenic variant, Progenitor cell
Clinical presentation	Healthy	Severe abnormal respiratory symptoms with bronchiectasis and abnormal lung function (reduced FEV$_1$)	Normal or mild respiratory symptoms
Immunofluorescence analysis to identify ODA defects	Normal DNAH5 localisation in all MCCs (normal ODA composition)	Abnormal DNAH5 localisation in all MCCs (abnormal ODA composition)	30–62% of MMCs show normal DNAH5 localisation (other MMCs exhibit ODA defects due to random X-chromosome inactivation)
In vitro ciliary clearance assay (in ALI cultures)	Healthy individuals show normal ciliary clearance transport	Male PCD individuals with hemizygous pathogenic variants in DNAAF6 show no *in vitro* ciliary clearance transport	Female carriers show directed ciliary clearance transport and reduced particle velocity
In vivo measurement of ciliary clearence (radioaerosol studies)	Tracheobronchial velocity (bolus transport): 2.0–6.0 mm·min^{-1} — Lung retention (24 h): normal	Tracheobronchial velocity (bolus transport): 0 mm·min^{-1} (severely abnormal) — Lung retention (24 h): abnormal	Tracheobronchial velocity (bolus transport): 1.7–3.0 mm·min^{-1} (slightly abnormal to normal) — Lung retention (24 h): slightly abnormal to normal
Conclusion	Normal ciliary clearance →	No ciliary clearance ✗→	Normal to slightly abnormal ciliary clearance → / A range of 30–62% of functioning multiciliated airway cells is sufficient to maintain ciliary airway clearance

GRAPHICAL ABSTRACT Overview of the study. PCD: primary ciliary dyskinesia; FEV$_1$: forced expiratory volume in 1 s; ODA: outer dynein arm; MCC: multiciliated cell.

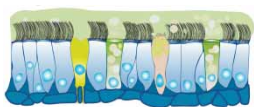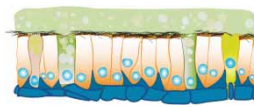# A range of 30–62% of functioning multiciliated airway cells is sufficient to maintain ciliary airway clearance

Niki T. Loges[1], June Kehlet Marthin [2,3], Johanna Raidt[1], Heike Olbrich[1], Inga M. Höben[1], Sandra Cindric[1], Diana Bracht[1], Julia König [1], Cynthia Rieck[1], Sebastian George[1], Tim Luis Kloth[1], Kai Wohlgemuth[1], Petra Pennekamp[1], Bernd Dworniczak[1], Mathias G. Holgersen [2], Jobst Römel [4], Christian Schmalstieg[1], Isabella Aprea[1], Jann Mortensen[2,5], Kim G. Nielsen[2,3] and Heymut Omran [1]

[1]Department of General Pediatrics, University Children's Hospital Muenster, Muenster, Germany. [2]Danish PCD Centre, Danish Paediatric Pulmonary Service, Department of Paediatrics and Adolescent Medicine, Rigshospitalet, Copenhagen University Hospital, Copenhagen, Denmark. [3]Department of Clinical Medicine, University of Copenhagen, Copenhagen, Denmark. [4]Department of Pediatric Respiratory Medicine, Immunology and Critical Care Medicine, Charité – Universitätsmedizin Berlin, Corporate Member of Freie Universität Berlin and Humboldt-Universität zu Berlin, Berlin, Germany. [5]Department of Clinical Physiology, Nuclear Medicine and PET, Rigshospitalet, Copenhagen University Hospital, Copenhagen, Denmark.

Corresponding author: Heymut Omran (Heymut.Omran@ukmuenster.de)

Abstract

Background Primary ciliary dyskinesia is a genetic disorder caused by aberrant motile cilia function that results in defective ciliary airway clearance and subsequently leads to recurrent airway infections and bronchiectasis. We aimed to determine: how many functional multiciliated airway cells are sufficient to maintain ciliary airway clearance?

Methods To answer this question we exploited the molecular defects of the X-linked recessive primary ciliary dyskinesia variant caused by pathogenic variants in *DNAAF6* (*PIH1D3*), characterised by immotile cilia in affected males. We carefully analysed the clinical phenotype and molecular defect (using immunofluorescence and transmission electron microscopy) and performed *in vitro* studies (particle tracking in air–liquid interface cultures) and *in vivo* studies (radiolabelled tracer studies) to assess ciliary clearance of respiratory cells from female individuals with heterozygous and male individuals with hemizygous pathogenic *DNAAF6* variants.

Results Primary ciliary dyskinesia male individuals with hemizygous pathogenic *DNAAF6* variants displayed exclusively immotile cilia, absence of ciliary clearance and severe primary ciliary dyskinesia symptoms. Owing to random or skewed X-chromosome inactivation in six female carriers with heterozygous pathogenic *DNAAF6* variants, 54.3±10% (range 38–70%) of multiciliated cells were defective. Nevertheless, *in vitro* and *in vivo* assessment of the ciliary airway clearance was normal or slightly abnormal. Consistently, heterozygous female individuals showed no or only mild respiratory symptoms.

Conclusions Our findings indicate that having 30–62% of multiciliated respiratory cells functioning can generate either normal or slightly reduced ciliary clearance. Because heterozygous female carriers displayed either no or subtle respiratory symptoms, complete correction of 30% of cells by precision medicine could improve ciliary airway clearance in individuals with primary ciliary dyskinesia, as well as clinical symptoms.

Introduction

The respiratory epithelium consists of different types of cells: non-ciliated cells (*e.g.* ionocytes, goblet and club cells) and ciliated cells. Coordinated beating of multiple motile cilia is essential for ciliary clearance of the upper and lower airways and represents an effective defence mechanism to prevent airway damage [1, 2]. Respiratory cilia characteristically beat with a forward effective stroke and a backward recovery

stroke in the same plane along the cell surface. Primary ciliary dyskinesia (PCD), listed in the Online Mendelian Inheritance in Man catalogue of human genes and genetic disorders under the number 244400, is a rare genetic heterogeneous disorder caused by aberrant motile cilia function. Dysfunction of motile cilia in the airway results in defective ciliary clearance of the upper and lower airways and subsequently leads to recurrent airway infections, chronic inflammation, bronchiectasis and progressive lung failure [2, 3]. Outer dynein arm (ODA) complexes attached at 24 nm intervals to the peripheral microtubule doublets contain molecular motors that drive and regulate ciliary motility, while the inner dynein arms (IDAs) regulate the ciliary and flagellar beating pattern. Dynein axonemal assembly factors (DNAAFs) are responsible for the cytoplasmic preassembly of ODAs and IDAs before transport to the ciliary axoneme [4, 5]. We and others have shown that pathogenic variants in *DNAAF6* cause the absence of all ODAs from the ciliary axonemes (shown by the absence of dynein axonemal heavy chain 5 (DNAH5)) as well as IDA defects (shown by the absence of dynein axonemal light intermediate chain 1 (DNALI1)) and therefore result in cilia immotility [6–8]. No causative treatment is thus far available and treatment efforts are aimed at hydration of mucus and early eradication of bacterial airway infections. Azithromycin maintenance therapy currently stands as the only evidence-based medical treatment within this context [9]. Precision medicine approaches in PCD, including gene therapy, mRNA transcript therapy and read-through therapy, are currently being explored [10].

However, it is not known how many multiciliated airway cells have to be completely corrected in order to restore ciliary airway clearance. To answer this very important medical and biological question, we exploited the molecular defects caused by pathogenic variants in the DNAAF gene *DNAAF6/PIH1D3*, responsible for a severe type of PCD characterised by immotile cilia in affected male individuals [6, 7]. Here, aberrant cytoplasmic assembly of axonemal ODAs and IDAs responsible for cilia beat generation and regulation causes complete ciliary immotility. We chose to explore the molecular defects underlying this X-linked model of PCD because X-chromosome inactivation (XCI) has evolved to equalise X-linked gene expression between female XX and male XY individuals to enable dosage compensation in marsupial and placental mammalians [11]. Failure to induce XCI in XX human embryos shows that a double dose of certain X-located genes results in early lethality during development [12]. In somatic tissues, the choice of which X chromosome to inactivate is generally random (figure 1). Because XCI is stably maintained, the same chromosome is inactivated in all progeny cells. Therefore, female individuals are mosaics of two populations of cells that differ in the X-chromosome that is active. Thus, in female individuals with heterozygous pathogenic *DNAAF6* variants, half of all ciliated respiratory cells are lined with immotile cilia, whereas male individuals with hemizygous pathogenic *DNAAF6* variants display exclusively immotile cilia in the airways (figure 1). However, skewed XCI can occur [13, 14] and even result in disease. For instance, in some female carriers of a dystrophin gene mutation, skewed inactivation (>90%) results in muscular dystrophy [15–17].

Here, we report five male PCD individuals with hemizygous and six female individuals with heterozygous pathogenic *DNAAF6* variants from four distinct families (figure 2). We identified three distinct large genomic deletions with variable sizes, a 10 kB deletion (exons 2–4 of *DNAAF6*), a 28 kB deletion (exon 1 of *DNAAF6*) and a 400 kB deletion (all *DNAAF6* exons), as well as the pathogenic DNA variant c.266c>A resulting in premature stop of translation (p.Trp89*). All male *DNAAF6*-affected individuals presented with typical PCD symptoms and variant respiratory cilia were immotile due to absence of ODAs and IDAs. Interestingly, we observed in the female heterozygous carriers that, due to random XCI, 38–70% of multiciliated respiratory cells displayed immotile cilia due to aberrant ODAs (absence of DNAH5) and IDAs (absence of DNALI1). We carefully examined the clinical phenotype of the female carriers of the heterozygous pathogenic *DNAAF6* variants and performed *in vivo* functional ciliary clearance analyses using radiolabelled tracer and *in vitro* ciliary clearance assays in air–liquid interface (ALI) cultures of ciliated respiratory cells. Hemizygous male PCD individuals did not have any *in vitro* or *in vivo* ciliary clearance. However, despite 38–70% of the respiratory ciliated cells carrying immotile cilia, female carriers with heterozygous pathogenic *DNAAF6* variants showed no or only mild respiratory symptoms. *In vitro* and *in vivo* ciliary clearance assays were either normal or showed a subtle reduction in ciliary clearance. We conclude that it is not necessary to have 100% of respiratory ciliated cells functioning to ensure effective ciliary clearance. A range of 30–62% of functioning cells is sufficient to provide either normal or only a subtle reduction in *in vitro* and *in vivo* ciliary clearance.

Material and methods

PCD-affected individuals and families

Signed and informed consent was obtained from individuals fulfilling the diagnostic criteria of PCD [18] and from family members according to protocols approved by the institutional ethics review board of the
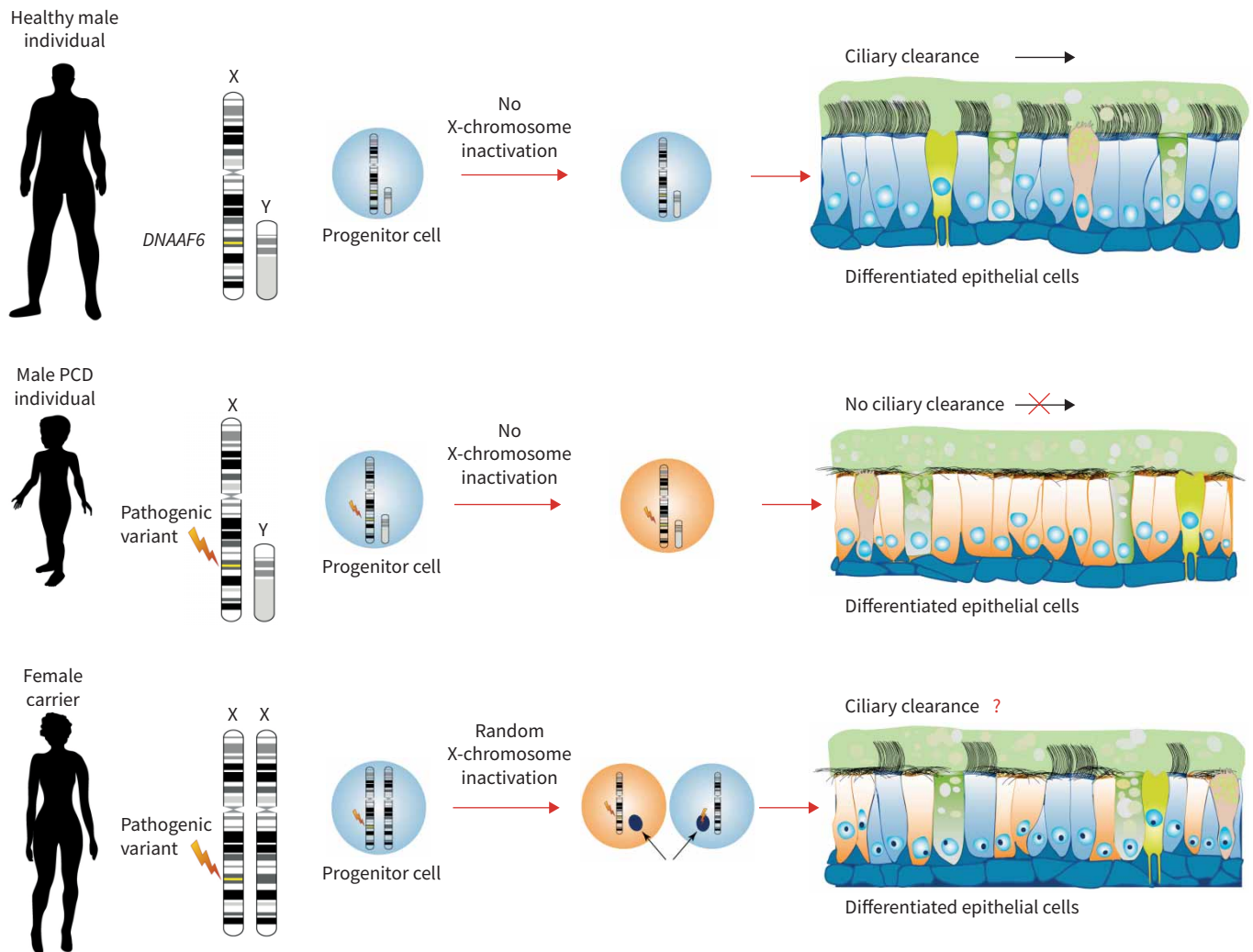
FIGURE 1 Random X-chromosome inactivation (XCI) in female carriers of heterozygous pathogenic *DNAAF6* variants results in two populations of respiratory ciliated cells. The differentiated respiratory epithelium consists of different type of cells: non-ciliated cells (*e.g.* ionocytes, goblet and club cells) and ciliated cells. *DNAAF6* is located on the X chromosome. In contrast to female individuals, in male individuals there is no XCI. Male individuals with a hemizygous pathogenic *DNAAF6* variant display exclusively immotile cilia in the airways, resulting in primary ciliary dyskinesia. In contrast, due to XCI, female individuals have a mosaic of two populations of cells that differ in the X-chromosome that is active. Thus, in female individuals with a heterozygous pathogenic *DNAAF6* variant, it is expected that half of all ciliated respiratory cells are lined with immotile cilia. In this study, we performed detailed *in vitro* and *in vivo* studies to assess the impact on ciliary clearance.

University Hospital Muenster (Ethik-Kommission Westfalen Lippe in Muenster, reference number 2015-104-f-S) and Copenhagen (Danish Data Protection Agency 2014).

Summary of applied methods
Please see the supplementary file for a detailed method section.

In this study, we performed mutational analyses using a customised PCD gene panel and whole exome sequencing (WES) and whole genome sequencing as well as Sanger sequencing to identify families with male PCD individuals carrying disease-causing hemizygous *DNAAF6* DNA variants (figure 2, supplementary figures S1–S4). Genetic variants were evaluated according to American College of Medical Genetics and Genomics (ACMG) and the Association for Molecular Pathology (AMP) guidelines [19]. We only report disease-causing (pathogenic) variants (class 5) according to ACMG/AMP guidelines. Further genetic analyses identified female heterozygous carriers of the *DNAAF6* variants (figure 2). Clinical findings such as laterality status and lung function and family history were ascertained (table 1).
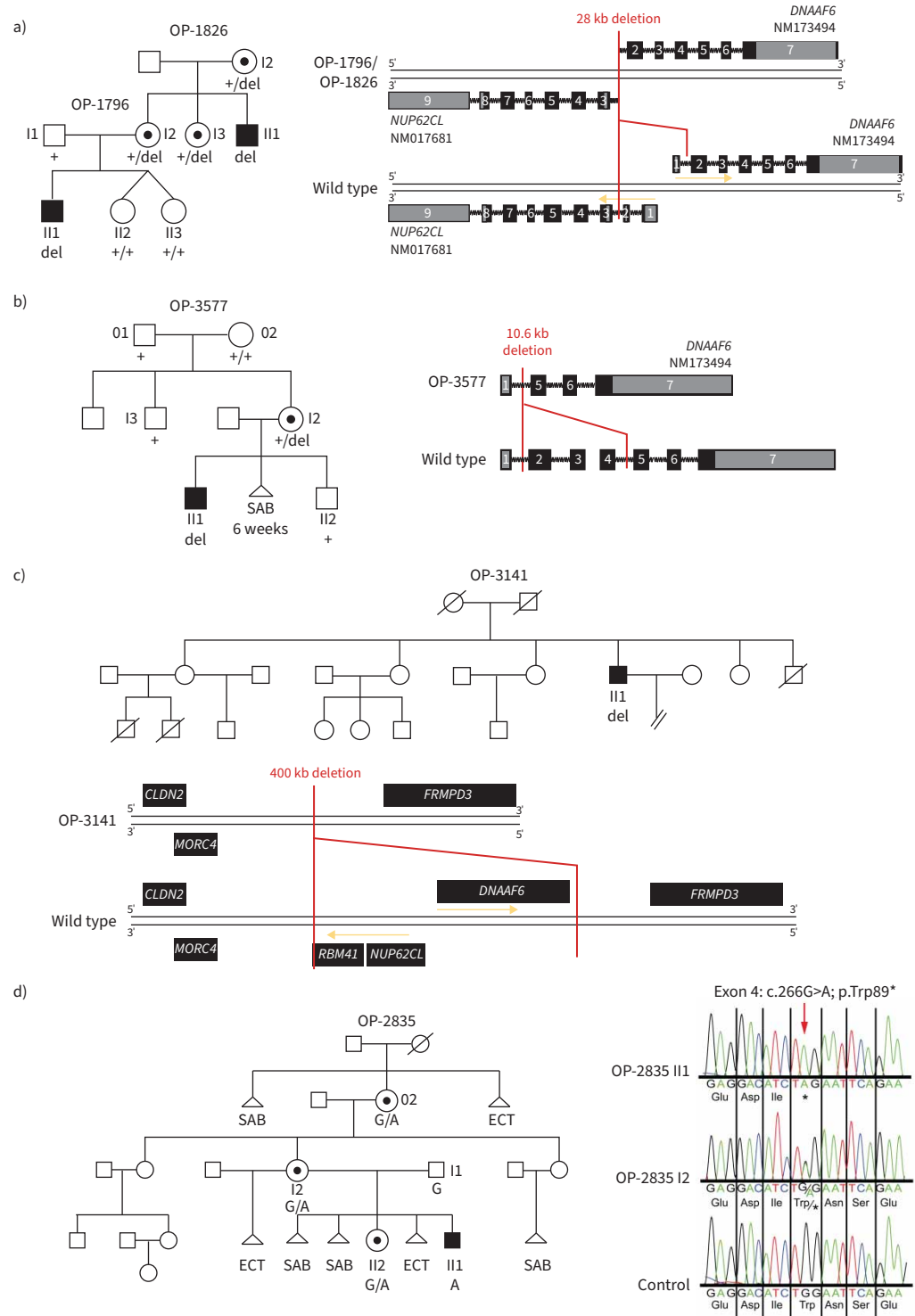
FIGURE 2 Pathogenic variants in *DNAAF6* located on the X chromosome were identified in four families. a) In family OP-1826/OP-1796 we found a 28 kb deletion (del) including the first exon of *DNAAF6* and the first two exons of *NUP62CL*. b) In family OP-3577, a 10.6 kb deletion comprising *DNAAF6* exons 2–4 was identified in OP-3577 I2. Segregation analyses revealed that neither her brother (OP-3577 I3) nor grandmother (OP-3577 02) carry the deletion, indicating that this is a *de novo* variant. OP-3577 I2 reported difficulties in getting pregnant and had one spontaneous abortion in the sixth week of pregnancy. c) In OP-3141 we identified a 400 kb deletion comprising *DNAAF6*, *NUP62CL* and *RBM41*. OP-3141 II1 is the fourth of six children. He has three older and one younger sister. The only brother died 10 days after birth owing to cardiorespiratory failure of unknown cause. His oldest sister gave birth to two male individuals: the first born died 3 months after birth, the second

born died 4 months after birth. Both died of unknown causes with cardiorespiratory failure. With another partner, she gave birth to a healthy boy. The second oldest sister has three healthy children, two girls and a boy. The third oldest sister gave birth to a healthy boy. The younger sister has no children. d) In family OP-2835, a transition from G to A (c.266G>A) was identified in *DNAAF6* exon 4, predicting premature stop of translation (p.Trp89*). Segregation analyses revealed that the mother (OP-2835 I2) and the grandmother (OP-2835 02) carry this variant in a heterozygous status whereas the father (OP-2835 I1) is unaffected. The great-grandmother of OP-2835 II1 had a spontaneous abortion (SAB) and gave birth to OP-2835 02, who inherited the *DNAAF6* variant. The great-grandmother died owing to complications of an ectopic (ECT) pregnancy. OP-2835 02 gave birth to three daughters. The oldest one has two healthy children, a girl, who already has another healthy daughter, and a boy. The second oldest one, OP-2835 I2, is a carrier of the *DNAAF6* variant and has two children. She had one ectopic pregnancy with a previous partner and with her current partner two spontaneous abortions and an ectopic pregnancy. OP-2835 II2 was her fourth pregnancy and is also a carrier of the *DNAAF6* variant. In addition, she gave birth to the index primary ciliary dyskinesia (PCD) male individual OP-2835 II1, who was her sixth pregnancy and who carries the hemizygous *DNAAF6* variant. The younger sister had one abortion and no children. PCD-affected males are shaded black and unaffected siblings are shaded white. Heterozygous female carriers are indicated by a central dot. Genotypes are indicated in the pedigrees.

To understand the molecular defects in the male hemizygous and female heterozygous *DNAAF6* variant individuals we performed various experiments in nasal ciliated airway cells (native cells after brushing), comprising transmission electron microscopy (TEM), high-speed video microscopy analysis (HVMA) and high-resolution immunofluorescence (IF) microscopy. We performed IF using antibodies directed against the ODA components DNAI1, DNAH5, DNAH9 and DNAI2 and the IDA component DNALI1. We counted a total of 500 cells per IF staining for male (n=1) and female (n=2) controls (OP-1796 I2, OP-1796 II1, OP-1826 I2, OP-1826 II1, OP-3577 I2 and OP-3577 II1). For OP-2835 II1, 200 cells and for OP-2835 I2 and OP-2835 II2 a total of 75 cells per IF staining and individual were counted. In addition ALI cultures from male hemizygous and female heterozygous *DNAAF6* variant individuals were established and the ciliary beat frequencies, ciliary particle transport, high-resolution IF and immunoblot analyses were performed. For ciliary particle transport measurements (*in vitro* ciliary clearance assay), fluorescent beads (0.5 and 2.0 µm in diameter) were mixed with pre-warmed cell culture medium and added to the apical compartment of respiratory cells in ALI culture (day 30 after airlift). Transport of fluorescent nanoparticles by ciliary beating was recorded using the Nikon Eclips Ti-S microscope (×20 objective lens) equipped with the NIS-Elements Advanced Research software (20 s; 7.5 frames·s^{-1}). In total, 30 videos per individual were analysed for statistical evaluation and 253 particles were tracked per video on average from three different cell culture inserts from each individual. Because two different bead sizes (0.5 and 2 µm) were used for the analyses, values were normalised against the mean value of the healthy control group. Tracking videos were evaluated using the NIS-Elements Advanced Research software (version 4.51.000) and NIS Advanced 2D Tracking plug-in to generate polargraphs and to determine the speed (µm·s^{-1}). In parallel to each recorded tracking video, a corresponding differential interference contrast (DIC) video was taken by an additionally equipped Basler sc640–120fm monochrome high-speed video camera (recording 125 frames·s^{-1}) to determine the cell condition as well as the ciliary beating pattern. DIC videos were evaluated using SAVA software [20]. Particle transport was measured in 18 healthy female individuals and one healthy male individual (age 25–60 years). The results of the experiments were quantified and statistically analysed using R (www.r-project.org).

To measure pulmonary ciliary clearance *in vivo*, we performed pulmonary radioaerosol mucociliary clearance (PRMC) measurements in one male PCD individual and three female carriers. For PRMC measurement, insoluble technetium-99m labelled nanocolloids were aerosolised and inhaled by 20 slow inspirations and successive forced expirations. Initial lung deposition and subsequent pulmonary mucociliary clearance immediately after inhalation of the radiolabelled tracer were assessed by repeated dynamic and static scintigraphic acquisitions for 2 h. In addition, a static measurement after 24 h and krypton-81m ventilation imagery of the ventilated lung area was performed. Whole-lung retention 1 h and 2 h after tracer inhalation were compared to predicted values calculated from penetration index, age and sex using previously published reference equations [21]. Tracheobronchial velocity (TBV) (bolus transport) was measured from dynamic acquisitions within the first hour. Involuntary cough was monitored by trained staff and significant coughing rendered the test inconclusive to avoid false positive PRMC results due to cough clearance. If a subject coughed during the test, voluntary cough clearance was assessed by 1 min of rigorous coughing after 2 h by analysing both the central part and the total lung regions [22].

TABLE 1 Clinical findings of female heterozygous pathogenic *DNAAF6* variant carriers and PCD males with hemizygous pathogenic *DNAAF6* variants

	OP-1796 I2	OP-1796 I3	OP-1826 I2	OP-2835 I2	OP-2835 II2	OP-3577 I2	OP-1796 II1	OP-1826 II1	OP-2835 II1	OP-3141 II1	OP-3577 II1
Gender	F	F	F	F	F	F	M	M	M	M	M
Age (years)	43	37	67	53	26	34	16	45	19	60	3
Origin	Denmark	Denmark	Denmark	Germany	Germany	Germany	Denmark	Denmark	Germany	Germany	Germany
Mutation in *DNAAF6*	28 kb deletion (het)	28 kb deletion (het)	28 kb deletion (het)	c.266G>A; p. Trp89* (het)	c.266G>A; p. Trp89* (het)	10.6 kb deletion (het)	28 kb deletion (hem)	28 kb deletion (hem)	c.266G>A; p. Trp89* (hem)	400 kb deletion (hem)	10.6 kb deletion (hem)
SI	No	No	No	No	No	No	No	No	No	No	Yes
Consanguinity	No	No	No	No	No	No	No	No	No	No	No
nNO (nL·min^{-1})	459	495	NA	241.7	55	122.1	9.6	19.8	29.7 (2017); 3 (2017); 16.1 (2019)	22.5	6.6
Lung function	Obstructive ppFEV$_1$: 87% ppFVC: 110% FEV$_1$/FVC: 64%	ppFEV1: 101% ppFVC: 116% FEV$_1$/FVC: 72%	ppFEV1: 115% ppFVC: 121% FEV$_1$/FVC: 73%	ppFEV1: 123% ppFVC: 130% FEV$_1$/FVC: 81%	Mild over blow, normal ppFEV$_1$: 111% ppFVC: 117% FEV$_1$/FVC: 83%	Overblow ppFEV$_1$: 101% ppFVC: 117% FEV$_1$/FVC: 76%	Obstructive/ restrictive ppFEV$_1$: 74% ppFVC: 117% FEV$_1$/FVC: 72%	Obstructive ppFEV$_1$: 69% ppFVC: 82% FEV$_1$/FVC: 66%	Mild over blow, normal ppFEV$_1$ 112%	Obstructive ppFEV$_1$ 46.5%	NA
Neonatal RDS	No	No	No	No	No	NA	Yes	Yes	Yes	NA	No
Chronic sinusitis	No	No	No	No	Yes	Yes	No	Yes	No	Yes	No
Chronic otitis media	No	No	No	No	Yes	No	Yes	Yes	Yes	Yes	No
Chronic bronchitis	No	Recurrent pneumonia	No	No	Yes (in childhood)	No	Yes	Yes	Yes	Yes	Yes
Chronic wet cough	No	Slight recurrent	No	No	No	No	Yes	Yes	Yes	Yes	Yes
Bronchiectasis	NA	No	NA	NA	NA	No	Yes	Yes	Yes	Yes	No
TEM	NA	67% ODA defect and 33% normal	NA	NA	NA	NA	ODA defect	ODA defect	NA	ODA defect	NA
IF	38% ODA defect and 62% normal 45% IDA defect and 55% normal	70% ODA defect and 30% normal 66% IDA defect and 34% normal	61% ODA defect and 39% normal 61% IDA defect and 39% normal	50% ODA defect and 50% normal 55% IDA defect and 45% normal	58% ODA defect and 42% normal 32% IDA defect and 68% normal	52% ODA defect and 48% normal 42% IDA defect and 58% normal	ODA/IDA defect	ODA/IDA defect	ODA/IDA defect	ODA/IDA defect	ODA/IDA defect
HVMA	Patches with motile and immotile cilia	Patches with motile and immotile cilia	Patches with motile and immotile cilia	Patches with motile and immotile cilia	Patches with motile and immotile cilia	Patches with motile and immotile cilia	Immotile	Immotile	Immotile	Immotile	Immotile
Fertility problems	No	No	No	Yes	NA	NA	NA	NA	NA	Yes	NA

F: female; hem: hemizygous; het: heterozygous; HVMA: high-speed video microscopy analyses; IF: high-resolution immunofluorescence microscopy; IDA: inner dynein arm; M: male; nNO: nasal nitric oxide production rate; NA: not available; ODA: outer dynein arm; ppFEV$_1$: % predicted forced expiratory volume in 1 s; ppFVC: % predicted forced vital capacity; RDS: respiratory distress syndrome; SI: *situs inversus*; TEM: transmission electron microscopy.

Results

High-resolution IF microscopy analyses

We performed high-resolution IF microscopy to analyse the ciliary defects at the cellular level in females with heterozygous and males with hemizygous pathogenic *DNAAF6* variants, respectively (figures 3 and 4). We used antibodies directed against ODA components DNAI1, DNAH5, DNAH9 and DNAI2. Analyses of ciliated respiratory cells from female heterozygous carriers (OP-1796 I2, OP-1796 I3, OP-1826 I2, OP-3577 I2, OP-2835 I2 and OP-2835 II2) revealed that 54.3±10% (range 38–70%, table 1) of ciliated respiratory cells showed abnormal localisation of the ODA components DNAI1, DNAH5, DNAH9 and DNAI2 (table 1, figures 3 and 5, and supplementary figures S5, S9, S11 and S13) when compared to control respiratory cells (1.8±0.67%), consistent with random XCI. However, some female carriers (*e.g.* OP-1769 I3) had a very low proportion of normal multiciliated cells (30%), whereas others (*e.g.* OP1796 I2) had a high proportion (62%), indicating that those carriers had a skewed XCI. In accordance with reported findings [6–8], we found no ODAs in analysed ciliated respiratory cells (99.8±0.37%) from male PCD individuals carrying hemizygous variants in *DNAAF6* (OP-1796 II1, OP-1826 II1, OP-3577 II1 and OP-2835 II1; figures 4 and 5, and supplementary figures S6, S10 and S12). Next, we analysed the localisation of the IDA component DNALI1. In female carriers, 45.2±13% (range 32–66%, table 1) of the respiratory cells showed abnormal localisation of DNALI1 along the ciliary axoneme when compared to control respiratory cells (2.4±1.6%) (figures 3 and 5, and supplementary figure S7). As expected, we observed an absence of DNALI1 in almost all respiratory cells (99.6±0.4%) from male PCD individuals carrying hemizygous variants in *DNAAF6* (figures 4 and 5, and supplementary figure S8). Statistical analysis using the ANOVA two-tailed test showed a significantly increased count of ODA-defective and IDA-defective cells in respiratory cell samples from female carriers with a heterozygous *DNAAF6* pathogenic variant when compared to healthy control respiratory cells ($p < 0.001$). In addition, there was a significantly increased count of cells with normal ODA/IDA composition in respiratory cell samples from female carriers with a heterozygous pathogenic *DNAAF6* variant when compared to male PCD individuals with a hemizygous pathogenic *DNAAF6* variant ($p < 0.001$). For male (n=1) and female (n=2) controls and for OP-1796 I2, OP-1796 I3, OP-1796 II1, OP-1826 I2, OP-1826 II1, OP-3577 I2 and OP-3577 II1, a total of 500 cells per IF staining were counted. For OP-2835II1, 200 cells were counted and for OP-2835 I2 and OP-2835 II2, 75 cells per IF staining were counted.

TEM

To further analyse the ciliary defect resulting from heterozygous pathogenic variants in *DNAAF6*, we performed TEM with samples from OP-1796 I3. In total, 581 ciliary axonemes were analysed. Our findings confirm that heterozygous pathogenic *DNAAF6* variants result in a mosaic of cells with and without axonemal ODA defects (figure 6 and supplementary figure S14). Furthermore, ultrastructural analyses found ciliary cross-sections without ODAs (n=391, 67%) but also ciliary cross-sections with normal ODA localisation (n=190, 33%), consistent with our IF microscopy findings (table 1) and skewed XCI in OP-1796 I3.

HVMA

HVMA of nasal respiratory epithelial cells to assess ciliary beating in male PCD individuals carrying hemizygous *DNAAF6* variants showed that all respiratory cells were lined with immotile cilia (supplementary videos 1 and 2), consistent with the observed axonemal ODA defects by IF microscopy (figure 4). In the female carriers, patches with motile and immotile cilia were observed (supplementary videos 3–7 and supplementary table S2), consistent with variable XCI and our IF microscopy findings. In OP-1796 I3, 340 of 597 (57%) multiciliated cells carried immotile cilia, consistent with skewed XCI and also supported by IF and TEM findings. In the other female carriers who were analysed by HVMA (OP-2835 II2 and OP-1826 I2), patches of multiciliated cells with motile and immotile cilia were observed. However, due to the low number of cells counted, no quantification was performed.

Measurement of ciliary clearance *in vitro and* in vivo

Next, we tested whether respiratory cilia of *DNAAF6*-mutant cells can generate a directed fluid flow. To mimic the process of ciliary clearance *in vitro*, we added fluorescent particles to the apical compartment of respiratory cells in ALI culture from healthy control individuals; female carriers OP-1796 I2, OP-1796 I3, OP-1826 I2 and OP-3577 I2 with the heterozygous pathogenic *DNAAF6* variant; and PCD male individuals OP-1796 II1, OP-1826 II1, OP-2835 II1 and OP-3141 II1 carrying hemizygous pathogenic *DNAAF6* variants. Consistent with PCD and aberrant ciliary clearance, mutant cilia from PCD male individuals with hemizygous pathogenic *DNAAF6* variants were not able to transport fluorescent particles along the surface of the differentiated epithelium (figure 7 and supplementary figure S15) and ciliary clearance significantly differed from healthy controls ($p = 0.0003$). In contrast, respiratory cilia from healthy controls and carriers of heterozygous pathogenic *DNAAF6* variants were able to generate a directed fluid flow (figure 7). However,
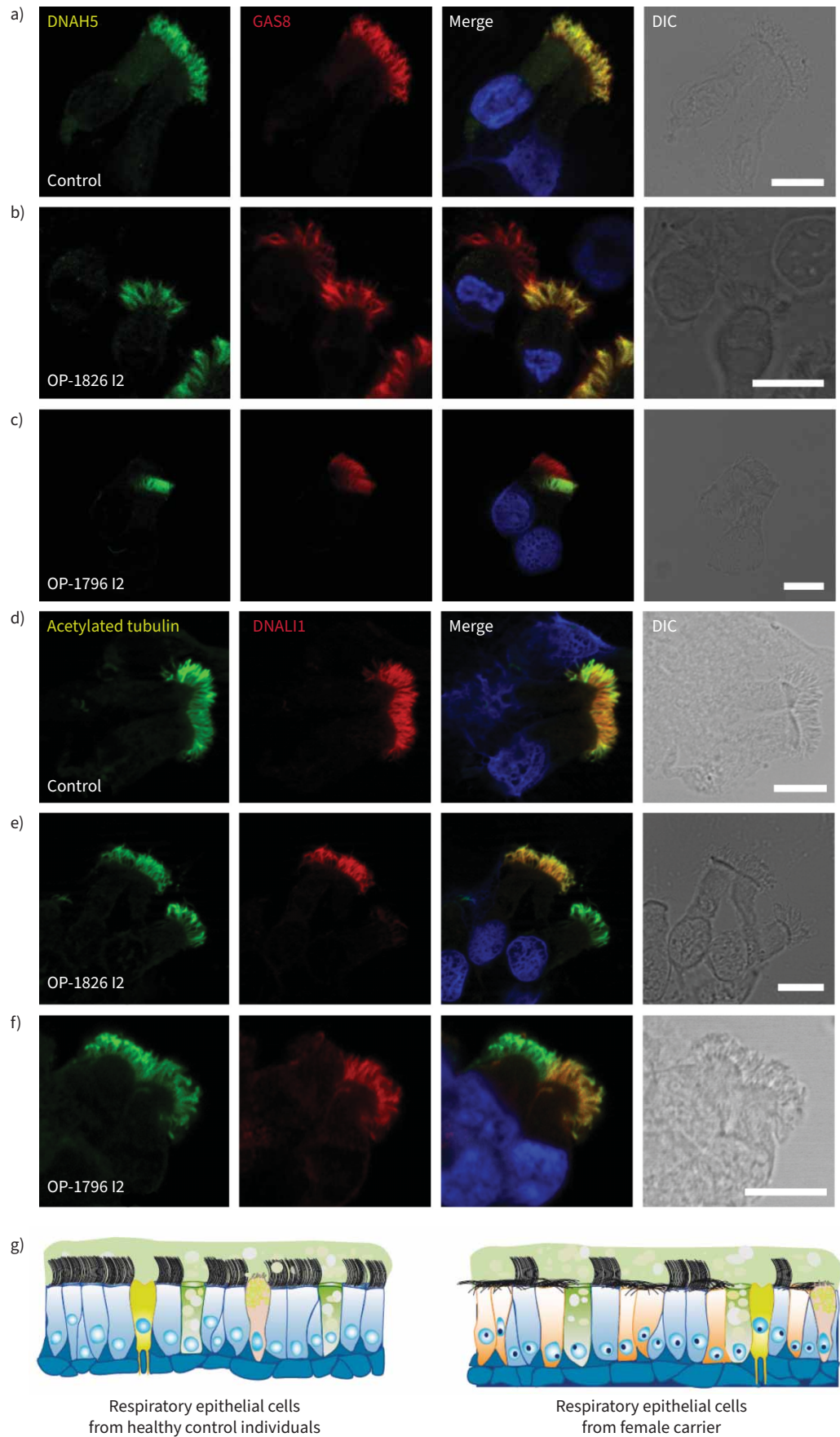
a) DNAH5 | GAS8 | Merge | DIC
Control

b) OP-1826 I2

c) OP-1796 I2

d) Acetylated tubulin | DNALI1 | Merge | DIC
Control

e) OP-1826 I2

f) OP-1796 I2

g)

Respiratory epithelial cells
from healthy control individuals

Respiratory epithelial cells
from female carrier

FIGURE 3 Heterozygous *DNAAF6* pathogenic variants in female individuals result in a mosaic of cells with and without axonemal outer and inner dynein arm defects, respectively. a–c) Respiratory epithelial cells from female control individuals and female carriers with a heterozygous pathogenic *DNAAF6* variant were double-labelled with antibodies directed against the outer dynein arm protein DNAH5 (green) and GAS8 (red). Both proteins colocalise (yellow) along the ciliary axonemes in all cells from the unaffected control (a). In female carriers with a heterozygous pathogenic *DNAAF6* variant, DNAH5 showed a normal localisation in some cells or was completely absent or severely reduced in the ciliary axonemes of other (b, c). d–f) Respiratory epithelial cells from a female control and female carriers with a heterozygous pathogenic *DNAAF6* variant were double-labelled with antibodies directed against acetylated tubulin (green) and the inner dynein arm protein DNALI1 (red). Both proteins colocalise (yellow) along the ciliary axonemes in all cells from the unaffected control (d). In female carriers with heterozygous pathogenic *DNAAF6* variant, DNALI1 showed a normal localisation in some cells or was completely absent or severely reduced in the ciliary axonemes of other cells (e, f). Nuclei were stained with Hoechst 33342 (blue). g) Schematic summarising the immunofluorescence microscopy results. In female control cells, cytoplasmic preassembly of dynein arms was not altered and all cells showed normal axonemal composition of inner (DNALI1) and outer (DNAH5) dynein arms. In contrast, female carriers with a heterozygous pathogenic *DNAAF6* variant show a mosaic of cells with normal axonemal composition of dynein arms (blue) and abnormal composition dynein arms (yellow), respectively. Scale bars: 10 µm. DIC: differential interference contrast.

the velocity of this flow was significantly slower than that of the healthy controls (p=0.009). Two female carriers (OP-1796 I2 and OP-3577 I2) had *in vitro* ciliary transport velocities in the lower normal range also consistent with IF findings. OP-1796 I3 showed the lowest *in vitro* ciliary transport velocity (figure 7), consistent with skewed XCI that was also supported by IF, TEM and HVMA findings. OP-1826 I2 also had low *in vitro* ciliary transport velocity, also consistent with IF findings.

To measure pulmonary ciliary clearance *in vivo*, we performed bronchoscintigraphy in the female carriers OP-1796 I2, OP-1796 I3 and OP-1826 I2 with a heterozygous pathogenic *DNAAF6* variant and in the PCD male individual OP-1796 II1 carrying a hemizygous pathogenic *DNAAF6* variant. In the heterozygous female carriers, PRMC showed lung retention in the lower range of normal limits, with retention in the airways during the first 2 h of examination that was normal (z-score <1.65). There was no sign of increased airway retention in OP-1796 I2, but abnormal retention in OP-1796 I3 and slightly abnormal retention in the right lung in OP-1826 I2 after 24 h (supplementary table S3). TBV (normal range: 2–6 mm·min^{-1}) was normal in OP-1796 I2 (2.5 mm·min^{-1}) and OP-1826I2 (3 mm·min^{-1}), but slightly abnormal in OP-1796 I3 (1.7 mm·min^{-1}) (supplementary table S3, supplementary figure S16 and supplementary video 9). The subjects did not cough during the test. Thus, female carriers OP-1796 I3 and OP-1826 I2 showed slightly reduced *in vivo* pulmonary mucociliary clearance consistent with the reduced *in vitro* ciliary clearance velocity, probably caused by skewed XCI. In contrast, PCD individual OP-1796 II1 had abnormal lung retention after 1 h, 2 h and 24 h (z-score >1.65) and a TBV of 0 mm·min^{-1} (supplementary video 10). Also, nasal mucociliary clearance (NMC) velocity was 0 mm·min^{-1} (supplementary table S3 and supplementary figure S14). In fact, there was limited mucus transport in periods without coughing, while coughing could partly compensate for the reduced ciliary clearance.

Please see the supplementary file for additional results.

Discussion

We and others previously described the first non-syndromic X-linked PCD variant caused by DNA variants in *PIH1D3/DNAAF6* [6, 7]. Through careful analyses of family pedigrees, we identified four additional families consistent with an X-linked inheritance pattern (figure 2). Using WES, targeted gene panel sequencing and Sanger sequencing, we identified additional deletions and point mutations in *DNAAF6* (figure 2). The 28 kb deletion identified in the family OP-1796/OP-1826 comprises the first noncoding exon of *DNAAF6* and the first two noncoding exons of the adjacent gene *NUP62CL* (figure 2a and supplementary figure S1). The deletions of the two noncoding exons of *PIH1D3/DNAAF6* were not detectable by WES. However, WES is frequently used for PCD diagnostics [23]. This finding has implications for genetic diagnostics because WES usually captures only coding exons of genes in a genomic region; deletion of noncoding exons that might affect further splicing will be missed. Geneticists should be aware of this problem.

All affected male PCD individuals carrying hemizygous *DNAAF6* variants showed typical PCD symptoms (table 1). HVMA and particle tracking analyses revealed immotile respiratory cilia that were not able to generate *in vitro* and *in vivo* ciliary clearance (figure 7, supplementary videos 1 and 2, supplementary table
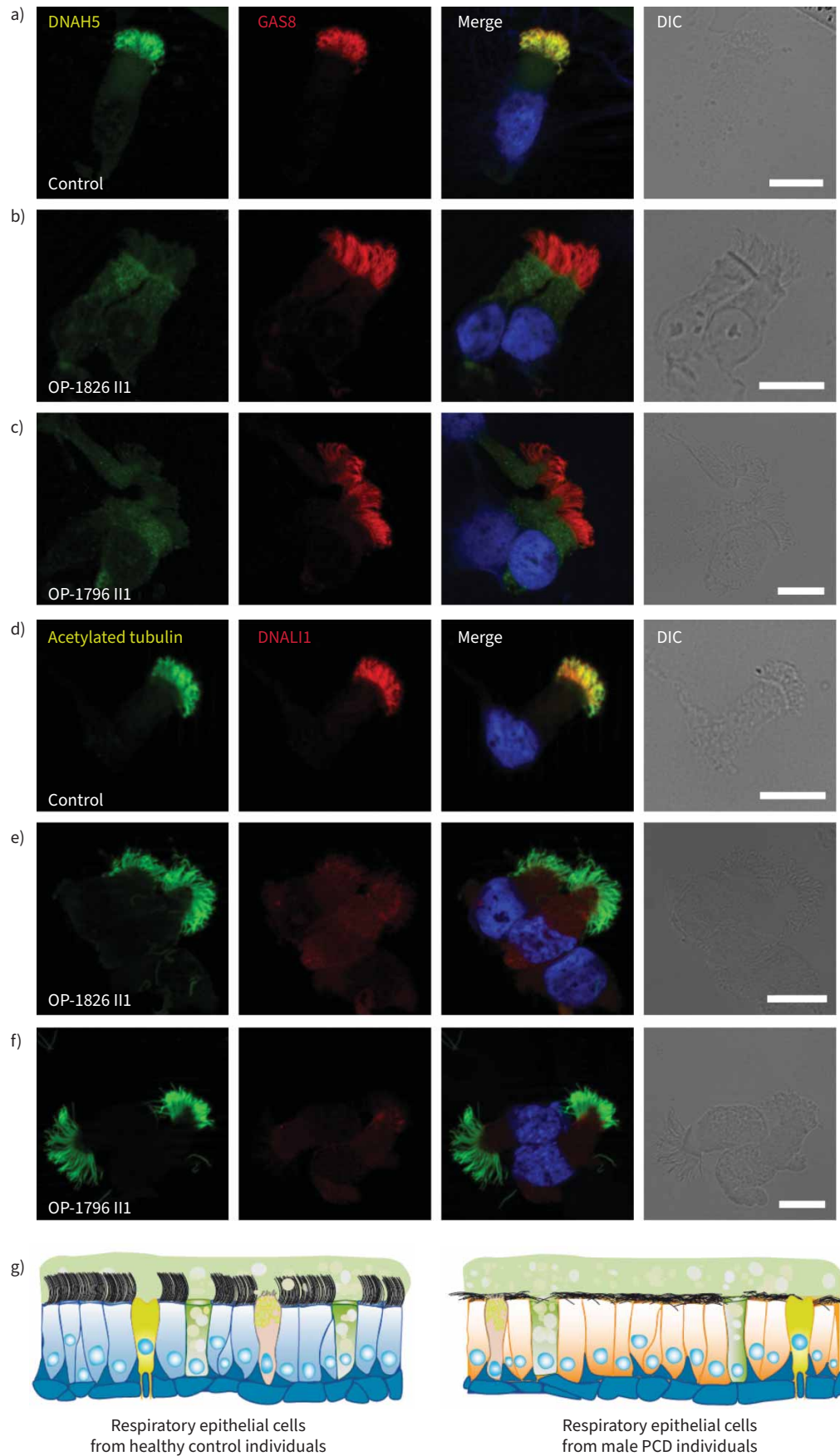
FIGURE 4 Hemizygous pathogenic variants in *DNAAF6* result in outer and inner dynein arm defects in primary ciliary dyskinesia (PCD)-affected males. a–c) Respiratory epithelial cells from control individuals and male PCD individuals OP-1826 II1 and OP-1796 II1 with a hemizygous pathogenic *DNAAF6* variant were double-labelled with antibodies directed against the outer dynein arm protein DNAH5 (green) and GAS8 (red). Both proteins colocalise (yellow) along the ciliary axonemes in cells from the unaffected control (a). In cells from PCD individuals OP-1826 II1 (b) and OP-1796 II1 (c), DNAH5 was completely absent or severely reduced from the ciliary axonemes of all cells analysed. d–f) Respiratory epithelial cells from a control and male PCD individuals OP-1826 II1 and OP-1796 II1 with hemizygous pathogenic *DNAAF6* variants were double-labelled with antibodies directed against acetylated tubulin (green) and the inner dynein arm protein DNALI1 (red). Both proteins colocalise (yellow) along the ciliary axonemes in all cells from the unaffected control (d). In cells from the male PCD individuals OP-1826 II1 (e) and OP-1796 II1 (f), DNALI1 was completely absent or severely reduced in the ciliary axonemes of all cells analysed. Nuclei were stained with Hoechst 33342 (blue). g) Schematic summarising the immunofluorescence microscopy results. In all control cells (blue), cytoplasmic preassembly of dynein arms was not altered and all cells showed normal axonemal composition of inner (DNALI1) and outer (DNAH5) dynein arms. In contrast, in male PCD individuals with hemizygous *DNAAF6* pathogenic variants, all cells show abnormal composition of dynein arms (yellow). Scale bars: 10 μm. DIC: differential interference contrast.

S3 and supplementary figure S16). IF microscopy findings are consistent with previous reports [6, 7]. Interestingly, three male infants died during early infancy due to unexplained cardiorespiratory failure (figure 2). Possibly, those infants had PCD and congenital heart disease or early respiratory failure. Early infant death in PCD has been reported but has not been studied in detail [24].

DNAAF6 is located on the X-chromosome and, in female individuals, one of their two X-chromosomes is transcriptionally silenced to compensate for a double dose of X-linked genes [25]. Consistent with variable XCI we found different degrees of defects in the multiciliated cells of the female carriers. IF microscopy
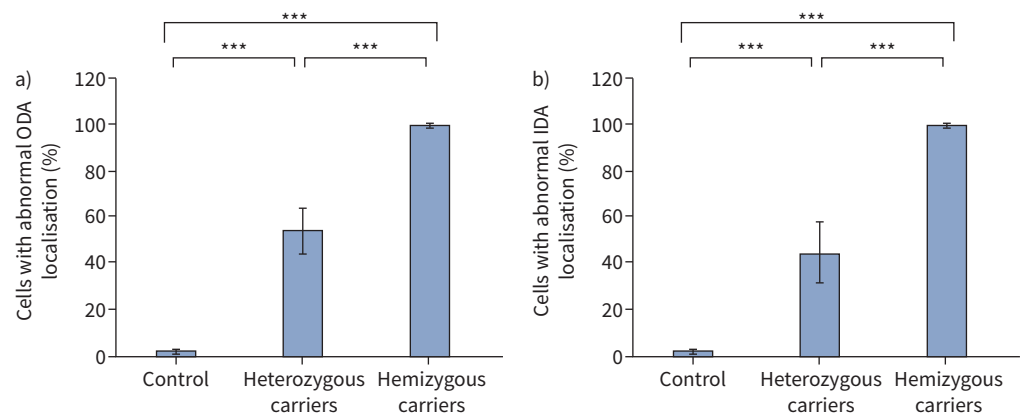

FIGURE 5 Pooled statistical analysis of immunofluorescence (IF) microscopy findings using antibodies directed against outer dynein arm (ODA) component DNAH5 (a) and the inner dynein arm (IDA) protein DNALI1 (b) in control respiratory cells, cells from female carriers with a heterozygous pathogenic *DNAAF6* variant (OP-1796 I2, OP-1796 I3, OP-1826 I2, OP-3577 I2 and OP-2835 I2) and male primary ciliary dyskinesia (PCD) individuals with a hemizygous pathogenic *DNAAF6* variant (OP-1796 II1, OP-1826 II1, OP-3577 II1, OP-2835 II1 and OP-2835 II2). a) Analyses of ciliated respiratory cells of females with a heterozygous pathogenic *DNAAF6* variant revealed that 54.3±10% (range 38–70%, table 1) show abnormal axonemal localisation of DNAH5 when compared to control respiratory cells (1.8±0.67%). In male PCD individuals with a hemizygous pathogenic *DNAAF6* variant, almost all respiratory cells showed absence of DNAH5 from the ciliary axonemes (99.8±0.37%). b) Analyses of ciliated respiratory cells of female carriers with a heterozygous *DNAAF6* pathogenic variant revealed that 45.2±13% (range 32–66%, table 1) show abnormal localisation of DNALI1 when compared to control respiratory cells (2.4±1.6%). In male PCD individuals with hemizygous pathogenic *DNAAF6* variants, almost all respiratory cells showed axonemal absence of DNALI1 (99.6±0.4%). For male (n=1) and female controls (n=2) and for OP-1796 I2, OP-1796 I3, OP-1796 II1, OP-1826 I2, OP-1826 II1, OP-3577 I2 and OP-3577 II1, a total of 500 cells per IF staining were counted. For OP-2835 II1, 200 cells were counted. For OP-2835 I2 and OP-2835 II2, 75 cells were counted. Error bars denote standard deviation. p-values were generated by the ANOVA two-tailed tests. ***: $p < 0.001$.
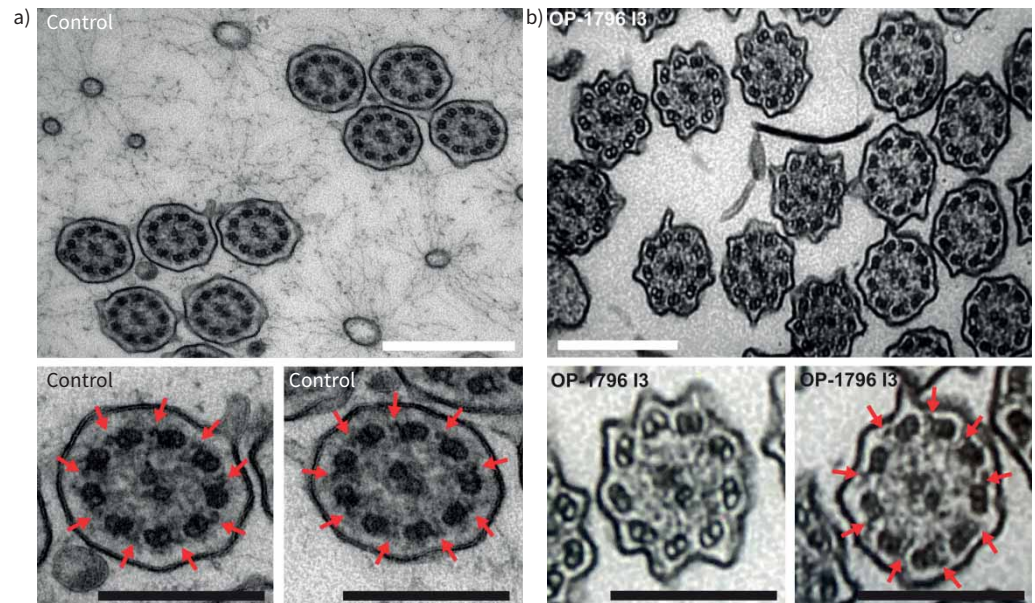
FIGURE 6 Heterozygous pathogenic *DNAAF6* variants in female carriers result in a mosaic of cells with and without axonemal outer dynein arm (ODA) defects. Transmission electron microscopy analysis of ciliary cross-sections from a) a control and b) female individual OP-1796 I3 carrying a heterozygous *DNAAF6* variant show the absence of ODAs in more than half of the ciliated cells (n=391 of 581 sections, 67%) from the female carrier. Red arrows mark ODAs. A total of 581 ciliary cross-sections from OP-1796 I3 were analysed. White scale bars: 500 nm; black scale bars: 250 nm.

showed that 38–70% of respiratory ciliated cells presented with an absence of ODAs and 32–66% presented with an absence of IDAs (table 1, figures 3 and 5 and supplementary figures S5, S7, S9, S11 and S13). *In vitro* measurement of ciliary clearance by particle tracking showed that the remaining functional cilia of the female carriers were able to generate a directed flow, contrasting with the findings in affected male individuals (no flow). However, flow was significantly slower than that of the healthy controls (p=0.009; figure 7). Two female carriers (OP-1796 I2 and OP-3577 I2) had *in vitro* ciliary transport velocities in the lower normal range consistent with IF findings. Individual OP-1796 I2 also had normal PRMC. However, OP-1796 I3 showed the lowest *in vitro* ciliary transport velocity (figure 7), consistent with skewed XCI and supported by IF, TEM and HVMA findings. OP-1826 I2 also had low *in vitro* ciliary transport velocity, also consistent with IF findings. OP-1796 I3 and OP-1826 I2 showed subtle abnormalities in *in vivo* PRMC (supplementary table S3). Interestingly, besides mild respiratory symptoms (table 1), female carriers did not have symptoms consistent with PCD. Only OP-1796 I3, who had the lowest proportion of functioning multiciliated cells (30% normal ODA composition), reported mild respiratory symptoms with chronic bronchitis, recurrent pneumonia and chronic wet cough (normal results on chest computed tomography).

The current BEAT PCD expert consensus guideline for TEM diagnosis considers the absence of ODAs in >50% of cross-sections as a class 1 hallmark defect pathognomonic for PCD [26]. Thus, our findings have implications for PCD diagnostics because by chance about half of female carriers will have more than 50% ODA-affected cilia, as present in OP-1796 I3 (figure 6 and supplementary figure S14). This is also consistent with our IF data showing that four of six female carriers had >50% abnormal cilia (table 1). The observed deviation of abnormal TEM (67%) and abnormal IF (70%) findings in the female carrier OP-1796 I3 probably resulted from a skewed XCI. This might also explain the differences in ciliary particle transport and in PRMC measurement observed between the female carriers.

Interestingly, female carriers of *DNAAF6* variants reported ectopic pregnancies and spontaneous abortions (figure 2). One woman died owing to complications of ectopic pregnancy. It has been speculated that, owing to dysfunction of motile cilia within the fallopian tubes, female PCD individuals might have an increased risk for infertility, ectopic pregnancies and spontaneous abortion. However, the few studies addressing this clinical finding in female PCD individuals could not support an increased risk [27, 28]. Our findings indicate that female *DNAAF6* carriers might carry a higher risk for ectopic pregnancies and spontaneous abortions.
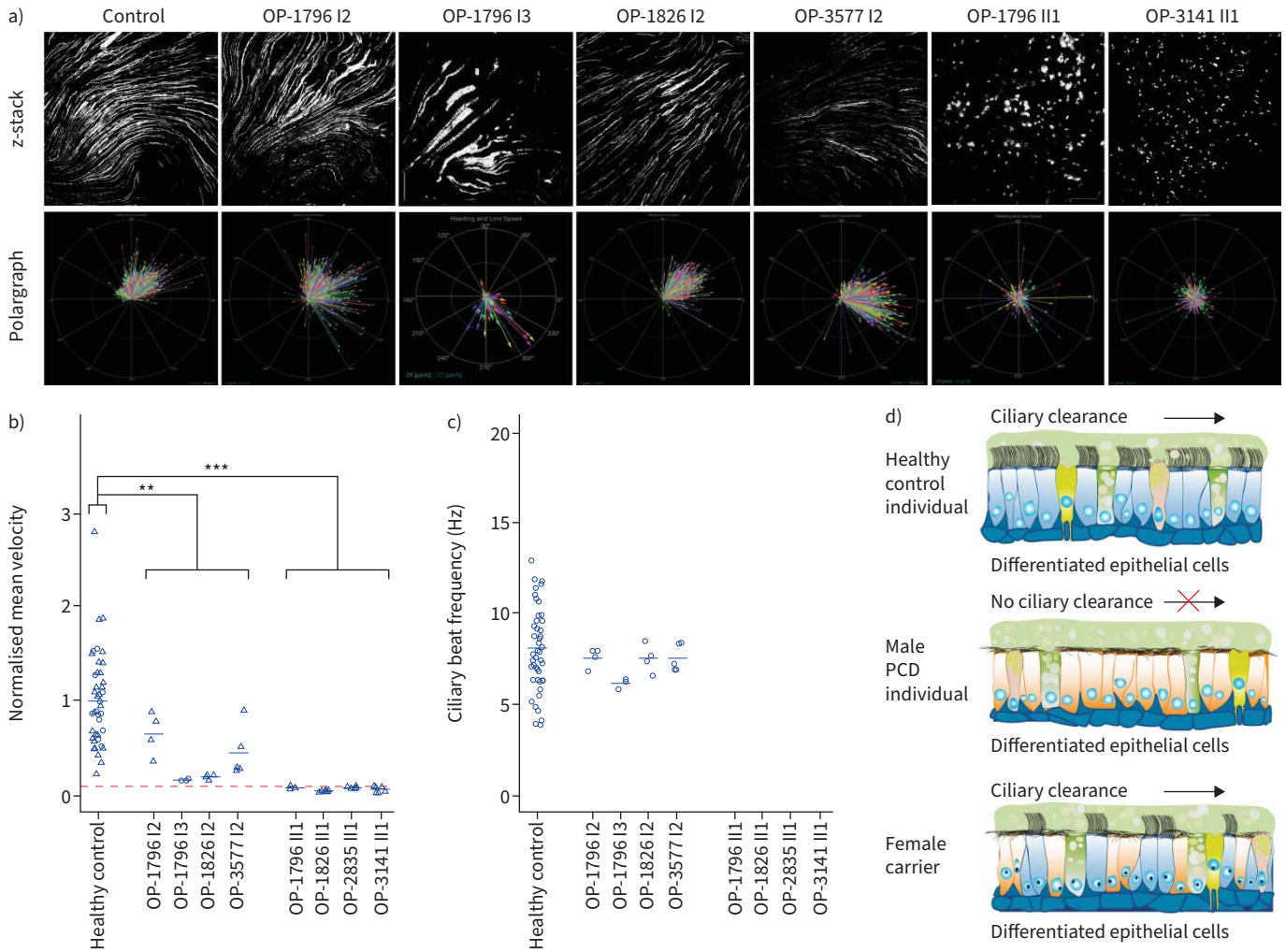
FIGURE 7 Air–liquid interface cultures of respiratory epithelial cells from female carriers with heterozygous pathogenic *DNAAF6* variants are able to generate a directed fluid flow while respiratory epithelial cells from male individuals with hemizygous pathogenic *DNAAF6* variants are unable to produce a fluid flow. a) After complete cell differentiation and ciliation (30 days after airlift), fluorescent particles were added to the apical compartments of the respiratory epithelial cells to assess ciliary clearance capacity. Tracking videos are represented as z-stack projections, while the transport direction of each particle is summarised in polargraphs. b) Respiratory cells from a control group (n=19) and female carriers with heterozygous pathogenic *DNAAF6* variants (OP-1796 I2, OP-1796 I3, OP-1826 I2 and OP-3577 I2) transported fluorescent particles in a linear direction along the cell layer. The velocity of this flow was significantly slower than that of the healthy controls (p=0.009, t-test). In contrast, the particle transport was non-oriented and significantly slower in male primary ciliary dyskinesia (PCD) individuals carrying hemizygous pathogenic *DNAAF6* variants (OP-1796 II1, OP-1826 II1, OP-2835 II1 and OP-3141 II1; p=0.0003, t-test). Circles indicate values measured with 2 µm beads while triangles indicate values measured with 0.5 µm beads. Because two different bead sizes were used for the analyses, values were normalised against the mean value of the healthy control group. Exact values are shown in supplementary figure S15. The significantly reduced particle transport measured in the male PCD individuals (dashed red line) is a thermal-driven background flow (Brownian movement). c) Measurement of the ciliary beat frequency of healthy controls (8.5 Hz), female carriers with heterozygous variants in *DNAAF6* (OP-1796 I2=7.6 Hz, OP-1796 I3=6.3 Hz, OP-1826 I2=7.7 Hz, OP-3577 I2=7.5 Hz) and male PCD individuals with hemizygous pathogenic *DNAAF6* variants (0 Hz). There was a subtle reduction in the ciliary beat frequency in female carriers with heterozygous *DNAAF6* variants compared to healthy controls (p=0.04, t-test). In total, 30 videos per individuals were analysed for statistical evaluation and 253 particles were tracked per video on average from three different cell culture inserts from each individual. d) Schematic summarising the particle tracking results. Ciliated cells from female control individuals (blue) were able to produce a directed flow. In contrast, in male PCD individuals with pathogenic *DNAAF6* variants (orange), all cells display cilia immotility due to lack of functional outer and inner dynein arms and the absence of directed particle transport.

A limitation to our study is the small number of individuals per group, especially for *in vivo* PRMC measurement (three heterozygous female carriers, one hemizygous PCD individual) because pathogenic variants in *DNAAF6* are rare.

Our results also suggest that clinical analyses of female carriers of heterozygous pathogenic *DNAAF6* variants should be considered in cases of respiratory symptoms consistent with PCD. It has been shown that skewness of XCI is relatively common and increases with age and can be tissue-specific [13, 14, 29, 30]. Therefore, skewed XCI can lead to an imbalanced inactivation of the wild-type X chromosome, resulting in more defective respiratory cilia which might cause PCD. Such an imbalanced inactivation of the wild-type X chromosome has previously been reported in female Duchenne muscular dystrophy patients [15–17]. Very recently, a study by THOMAS *et al.* [31] showed that in female carriers of pathogenic *DNAAF6* variants, skewed inactivation (80%) results in PCD symptoms, in one case even causing bronchiectasis. In our study, in one female carrier (OP-1796 I3) we found 70% of cells were defective. This female carrier presented slightly abnormal bolus transport measured by PRMC and mild respiratory symptoms (table 1 and supplementary table S3) but no bronchiectasis, indicating that having 30% of ciliated respiratory cells functioning might be sufficient to provide ciliary clearance of the airway to avoid severe PCD symptoms. Based on the published findings and our findings, clinical monitoring of female carriers of variants in *DNAAF6* should be considered because skewness of XCI increases with age [26, 27].

Hemizygous male PCD individuals did not have any *in vitro* or *in vivo* ciliary clearance. However, despite 38–70% of the respiratory ciliated cells of female heterozygous pathogenic *DNAAF6* variant carriers having immotile cilia, these individuals showed no or only mild respiratory symptoms. We conclude that it is not necessary to have 100% of respiratory multiciliated cells functioning to ensure effective ciliary clearance. A range of 30–62% of multiciliated cells functioning is sufficient to provide either normal or only a subtle reduction in *in vitro* and *in vivo* ciliary clearance. Thus, precision medicine approaches probably do not have to completely correct all multiciliated airway cells to improve ciliary clearance in PCD caused by pathogenic *DNAAF6* variants.

References

1 Fliegauf M, Benzing T, Omran H. When cilia go bad: cilia defects and ciliopathies. *Nat Rev Mol Cell Biol* 2007; 8: 880–893.

2 Wallmeier J, Nielsen KG, Kuehni CE, *et al.* Motile ciliopathies. *Nat Rev Dis Primers* 2020; 6: 77.

3 Nielsen KG, Holgersen MG, Crowley S, *et al.* Chronic airway disease in primary ciliary dyskinesia-spiced with geno-phenotype associations. *Am J Med Genet C Semin Med Genet* 2022; 190: 20–35.

4 Desai PB, Dean AB, Mitchell DR. Cytoplasmic preassembly and trafficking of axonemal dyneins. *In:* King SM, ed. Dyneins: Structure, Biology and Disease (Second Edition). London, Academic Press, 2018; pp. 140–161.

5 Braschi B, Omran H, Witman GB, *et al.* Consensus nomenclature for dyneins and associated assembly factors. *J Cell Biol* 2022; 221: e202109014.

6 Paff T, Loges NT, Aprea I, *et al.* Mutations in *PIH1D3* cause X-linked primary ciliary dyskinesia with outer and inner dynein arm defects. *Am J Hum Genet* 2017; 100: 160–168.

7 Olcese C, Patel MP, Shoemark A, *et al.* X-linked primary ciliary dyskinesia due to mutations in the cytoplasmic axonemal dynein assembly factor *PIH1D3*. *Nat Commun* 2017; 8: 14279.

8 Aprea I, Raidt J, Höben IM, *et al.* Defects in the cytoplasmic assembly of axonemal dynein arms cause morphological abnormalities and dysmotility in sperm cells leading to male infertility. *PLoS Genet* 2021; 17: e1009306.

9   Kobbernagel HE, Buchvald FF, Haarman EG, et al. Efficacy and safety of azithromycin maintenance therapy in primary ciliary dyskinesia (BESTCILIA): a multicentre, double-blind, randomised, placebo-controlled phase 3 trial. *Lancet Respir Med* 2020; 8: 493–505.

10   Paff T, Omran H, Nielsen KG, et al. Current and future treatments in primary ciliary dyskinesia. *Int J Mol Sci* 2021; 22: 9834.

11   Graves JA. Evolution of vertebrate sex chromosomes and dosage compensation. *Nat Rev Genet* 2016; 17: 33–46.

12   Galupa R, Heard E. X-chromosome inactivation: a crossroads between chromosome architecture and gene regulation. *Annu Rev Genet* 2018; 52: 535–566.

13   Shvetsova E, Sofronova A, Monajemi R, et al. Skewed X-inactivation is common in the general female population. *Eur J Hum Genet* 2019; 27: 455–465.

14   Sharp A, Robinson D, Jacobs P. Age- and tissue-specific variation of X chromosome inactivation ratios in normal women. *Hum Genet* 2000; 107: 343–349.

15   Giliberto F, Radic CP, Luce L, et al. Symptomatic female carriers of Duchenne muscular dystrophy (DMD): genetic and clinical characterization. *J Neurol Sci* 2014; 336: 36–41.

16   Schänzer A, Rau I, Kress W, et al. Duchenne muscular dystrophy in a 4-year-old girl due to heterozygous frame shift deletion of the dystrophin gene and skewed X-inactivation. *Klin Padiatr* 2012; 224: 256–258.

17   Carsana A, Frisso G, Intrieri M, et al. A 15-year molecular analysis of DMD/BMD: genetic features in a large cohort. *Front Biosci (Elite Ed)* 2010; 2: 547–558.

18   Lucas JS, Barbato A, Collins SA, et al. European Respiratory Society guidelines for the diagnosis of primary ciliary dyskinesia. *Eur Respir J* 2017; 49: 1601090.

19   Richards S, Aziz N, Bale S, et al. Standards and guidelines for the interpretation of sequence variants: a joint consensus recommendation of the American College of Medical Genetics and Genomics and the Association for Molecular Pathology. *Genet Med* 2015; 17: 405–424.

20   Sisson JH, Stoner JA, Ammons B, et al. All-digital image capture and whole-field analysis of ciliary beat frequency. *J Microsc* 2003; 211: 103–111.

21   Mortensen J, Lange P, Nyboe J, et al. Lung mucociliary clearance. *Eur J Nucl Med* 1994; 21: 953–961.

22   Marthin JK, Holgersen MG, Nielsen KG, et al. Pulmonary radioaerosol mucociliary clearance assessment: searching for genotype-specific differences and potential as an outcome measure in primary ciliary dyskinesia. *ERJ Open Res* 2023; 9: 00685-2023.

23   Gileles-Hillel A, Mor-Shaked H, Shoseyov D, et al. Whole-exome sequencing accuracy in the diagnosis of primary ciliary dyskinesia. *ERJ Open Res* 2020; 6: 00213-2020.

24   Harrison MJ, Shapiro AJ, Kennedy MP. Congenital heart disease and primary ciliary dyskinesia. *Paediatr Respir Rev* 2016; 18: 25–32.

25   Lyon MF. Gene action in the X-chromosome of the mouse (*Mus musculus* L.). *Nature* 1961; 190: 372–373.

26   Shoemark A, Boon M, Brochhausen C, et al. International consensus guideline for reporting transmission electron microscopy results in the diagnosis of primary ciliary dyskinesia (BEAT PCD TEM Criteria). *Eur Respir J* 2020; 55: 1900725.

27   Raidt J, Werner C, Menchen T, et al. Ciliary function and motor protein composition of human fallopian tubes. *Hum Reprod* 2015; 30: 2871–2880.

28   Vanaken GJ, Bassinet L, Boon M, et al. Infertility in an adult cohort with primary ciliary dyskinesia: phenotype–gene association. *Eur Respir J* 2017; 50: 1700314.

29   Christensen K, Kristiansen M, Hagen-Larsen H, et al. X-linked genetic factors regulate hematopoietic stem-cell kinetics in females. *Blood* 2000; 95: 2449–2451.

30   Mengel-From J, Lindahl-Jacobsen R, Nygaard M, et al. Skewness of X-chromosome inactivation increases with age and varies across birth cohorts in elderly Danish women. *Sci Rep* 2021; 11: 4326.

31   Thomas L, Cuisset L, Papon JF, et al. Skewed X-chromosome inactivation drives the proportion of *DNAAF6*-defective airway motile cilia and variable expressivity in primary ciliary dyskinesia. *J Med Genet* 2024; 61: 595–604.